Role of posterodorsal medial amygdala urocortin-3 in pubertal timing in female mice

Deyana Ivanova[1], Xiao-Feng Li[1], Yali Liu[2], Caitlin McIntyre[1], Cathy Fernandes[3,4], Geffen Lass[1], Lingsi Kong[1] and Kevin T O'Byrne[1]

[1]Department of Women and Children's Health, Faculty of Life Science and Medicine, King's College London, UK

[2]Department of Assisted Reproduction, Shanghai Ninth People's Hospital, Shanghai Jiaotong University School of Medicine, Shanghai, People's Republic of China.

[3]Social, Genetic & Developmental Psychiatry Centre, Institute of Psychiatry, Psychology & Neuroscience, King's College London, UK

[4] MRC Centre for Neurodevelopmental Disorders, King's College London, UK

Corresponding author's contact details: Deyana Ivanova (deyana.ivanova@kcl.ac.uk; https://orcid.org/0000-0003-1508-166X) and Kevin T O'Byrne (kevin.obyrne@kcl.ac.uk; https://orcid.org/0000-0002-2548-4182), Department of Women and Children's Health, School of Life Course and Population Sciences, Faculty of Life Science and Medicine, King's College London, 2.92W Hodgkin Building, Guy's Campus, London SE1 1UL, UK.

Reprint requests: Deyana Ivanova, Department of Women and Children's Health, School of Life Course Sciences, Faculty of Life Science and Medicine, King's College London, 2.92W Hodgkin Building, Guy's Campus, London SE1 1UL, UK.

Abstract

Post-traumatic stress disorder impedes pubertal development and disrupts pulsatile LH secretion in humans and rodents. The posterodorsal sub-nucleus of the medial amygdala (MePD) is an upstream modulator of the hypothalamic gonadotropin-releasing hormone (GnRH) pulse generator, pubertal timing, as well as emotional processing and anxiety. Psychosocial stress exposure alters neuronal activity within the MePD increasing the expression of Urocortin3 (Ucn3) and its receptor corticotropin-releasing factor type-2 receptor (CRFR2) while enhancing the inhibitory output from the MePD to key hypothalamic reproductive centres. We test the hypothesis that psychosocial stress, processed by the MePD, is relayed to the hypothalamic GnRH pulse generator to delay puberty in female mice. We exposed C57Bl6/J female mice to the predator odor, 2,4,5-Trimethylthiazole (TMT), during pubertal transition and examined the effect on pubertal timing, pre-pubertal LH pulses and anxiety-like behaviour. Subsequently, we virally infected Ucn3-cre-tdTomato female mice with stimulatory DREADDs targeting MePD Ucn3 neurons and determined the effect on pubertal timing and pre-pubertal LH pulse frequency. Exposure to TMT during pubertal development delayed puberty, suppressed pre-pubertal LH pulsatility and enhanced anxiety-like behaviour, while activation of MePD Ucn3 neurons reduced LH pulse frequency and delayed puberty. Early psychosocial stress exposure decreases GnRH pulse generator frequency delaying puberty while inducing anxiety-behaviour in female mice, an effect potentially involving Ucn3 neurons in the MePD.

39 **Introduction**

40 In humans post-traumatic stress disorder (PTSD) is associated with altered pubertal timing and
41 the development of anxiety disorders (1,2). Predator odor exposure is a classic model for PTSD
42 in rodents (3) and has been shown to delay puberty (4), suppress luteinizing hormone (LH)
43 pulse frequency (5) and inhibit the pre-ovulatory LH surge (6). The gonadotropin-releasing
44 hormone (GnRH) pulse generator that controls the hypothalamus-pituitary-gonadal (HPG) axis
45 and pubertal development is restrained in the juvenile, but reactivated at a critical time point
46 with increased frequency leading to the initiation of puberty (7). However, the neural
47 mechanisms controlling pubertal timing are not fully established.

48 Kisspeptin (kiss1) is known to be a major gatekeeper of pubertal onset. An absence of the
49 *kiss1* gene and kiss1 receptor (kiss1r) in mice and humans leads to a loss of gonadal maturation
50 and a lack of pubertal onset (8,9), and treatment with kisspeptin can reactivate the HPG axis
51 during the juvenile hiatus in monkeys and rats (10,11). Kiss1 neurons are located in the
52 anteroventral periventricular nucleus (AVPV) and arcuate nucleus (ARC) of the hypothalamus
53 in mice (12). The ARC kiss1 neurons, known as KNDy because they co-express neurokinin B
54 (NKB) and dynorphin A (Dyn), are a critical component of the GnRH pulse generator (12–14).
55 The activation of KNDy neurons induces pulsatile release of kiss1 acting on GnRH dendrons
56 in the median eminence to stimulate pulsatile GnRH secretion (15). The AVPV kiss1 neurons
57 project to GnRH cell bodies and proximal dendrites and are known to control the preovulatory
58 LH surge and ovulation in rodents (16). In the juvenile, a neurobiological break exerted on the
59 ARC GnRH pulse generator suppresses pulsatile kiss1 release in the median eminence,
60 however the nature of this upstream inhibition of the GnRH pulse generator, which is released
61 at the end of the juvenile phase to trigger puberty is unknown (7).

62 The amygdala, a stress-sensitive part of the limbic brain, is involved in processing anxiety and
63 fear as well as modulating pubertal timing and the HPG axis. Lesioning of the amygdala

64 advances menarche in female rhesus macaques (17), whereas electrical stimulation of this
65 region delays puberty in rats (18). Specific lesioning of the posterodorsal sub-nucleus of the
66 medial amygdala (MePD) advances puberty in rats (19), suggesting this region may play a key
67 role in exerting an inhibitory break on pubertal timing. The MePD sends GABAergic
68 projections to various hypothalamic reproductive centres (20,21) and has been shown to project
69 directly to ARC KNDy neurons, although their neurochemical phenotype is undetermined
70 (22,23). Interestingly, the MePD contains a kiss1 neuronal population (24) and antagonism of
71 MePD kiss1 delays puberty, disrupts estrous cyclicity and the LH surge in rats (25). Moreover,
72 selective optogenetic stimulation of MePD kiss1 neurons increases LH pulse frequency in mice
73 (26). The MePD is highly responsive to psychosocial stress, exhibiting a distinct firing pattern
74 in response to predator odor (27) and recently cat odor was found to delay puberty, disrupt
75 estrous cyclicity and induce a fear response in rats (4). The MePD may be a central hub
76 involved in the integration of external olfactory and anxiogenic signals with the GnRH pulse
77 generator.

78 Central administration of the stress neuropeptide corticotrophin releasing factor (CRF) dose-
79 dependently delays puberty, while CRF-receptor antagonism advances puberty in rats (28).
80 Urocortin-3 (Ucn3), a member of the CRF family and an endogenous ligand for CRF type 2
81 receptors (CRFR2) is found in abundance in the MePD (29). Psychosocial stressors, including
82 social defeat and restraint, increase cfos expression in CRFR2 positive neurons and increase
83 Ucn3 mRNA expression in the MePD of rodents (30). Moreover, we have recently shown that
84 MePD Ucn3 mediates predator odor and restraint stress-induced suppression of pulsatile LH
85 secretion in mice (5).

86 In this study, we aimed to determine whether chronic predator odor stress exposure suppresses
87 pre-pubertal LH pulse frequency and delays pubertal timing in female mice. Additionally, we
88 assessed social, anxiety and fear-like behaviour as measures of psychosocial stress in predator

89 odor-exposed pre-pubertal female mice. Finally, we aimed to determine whether MePD Ucn3
90 signalling is involved in modulating pre-pubertal LH pulse frequency and pubertal timing in
91 female mice.

92 **Materials and Methods**

93 **Mice**

94 Breeding pairs of C57Bl6/J mice were purchased from Charles River Laboratories
95 International, Inc. For Ucn3-cre mice, cryopreserved sperm of strain (Tg(Ucn3-
96 cre)KF43Gsat/Mmucd; congenic on C57BL/6 background) was acquired from MMRRC
97 GENSAT. Breeding pairs of heterozygous transgenic Ucn3-cre mice were recovered by
98 insemination of female C57Bl6/J mice at King's College London. Genotyping of Ucn3-cre
99 mice was performed using PCR to detect heterozygosity. Heterozygous Ucn3-cre mice were
100 bred with cre-activated tdTomato reporter mice (strain B6.Cg-Gt(ROSA)26Sortm9(CAG-
101 tdTomato)Hze/J; congenic on C57BL/6 background obtained from The Jackson Laboratory,
102 Bar Harbor, ME, USA) to obtain Ucn3-cre-tdTomato mice, as previously described (5,29).
103 Litter size was reduced to 6-8 pups 2-3 days after birth (on pnd 2-3) to standardise body weight,
104 which can alter pubertal development. Mice aged between 21 to 45 days were group housed
105 in individually ventilated cages equipped with wood-chip bedding and nesting material with
106 food and water ad libitum and sealed with a HEPA-filter at 25 ± 1 °C in a 12:12 h light/dark
107 cycle, lights on at 07:00 h. All procedures were carried out following the United Kingdom
108 Home Office Regulations and approved by the Animal Welfare and Ethical Review Body
109 Committee at King's College London.

110 **Stereotaxic adeno-associated-virus injection**

111 All surgical procedures were carried out with aseptic conditions and under general anaesthesia
112 using ketamine (Vetalar, 100 mg/kg, i.p.; Pfizer, Sandwich, UK) and xylazine (Rompun, 10
113 mg/kg, i.p.; Bayer, Leverkusen, Germany). The mouse brain atlas of Paxinos and Franklin
114 (31) was used to obtain target coordinates for the MePD (2.15 mm lateral, -1.25 mm from
115 bregma, at a depth of -5.30 mm below the skull surface) of pre-pubertal mice. Mice at pnd 14
116 were temporarily taken from their mother and secured in a David Kopf stereotaxic frame (Kopf
117 Instruments), a small skin incision was made to reveal the skull and two small holes were
118 drilled above the location of the MePD. Bilateral stereotaxic viral injections of the stimulatory
119 adeno-associated-virus (AAV) carrying the DIO-hM3D-mCitrine, DREADD, construct
120 (AAV-hSyn-DIO-HA-hM3D(Gq)-IRES-mCitrine, $3x10^{11}$ GC/ml, Serotype:5; Addgene) was
121 administered intra-MePD using the robot stereotaxic system (Neurostar, Tubingen, Germany),
122 performed for the targeted expression of DIO-hM3D-mCitrine in MePD Ucn3 neurons in
123 Ucn3-cre-tdTomato mice. AAV-hSyn-DIO-HA-hM3D(Gq)-IRES-mCitrine (150 nl) was
124 bilaterally injected into the MePD using a 2-µl Hamilton micro syringe (Esslab, Essex, UK)
125 over 10 min and the needle was left in position for a further 5 min then slowly lifted over 2
126 min. Mice that were cre-positive received the AAV-hM3D injection (test mice) or a control
127 virus AAV-YFP (Addgene) (control mice) where the control virus does not contain the DIO-
128 hM3D-mCitrine construct. The mice were placed back with the mother for a further 7 days
129 until wean day (pnd 21). Nine Ucn3-cre-tdTomato mice received the AAV-hM3D injection,
130 6 Ucn3-cre-tdTomato mice received the control AAV-YFP, 4 Ucn3-cre-negative mice without
131 surgery received only CNO and 3 Ucn3-cre-tdTomato mice without surgery did not receive
132 CNO.

133 **Chronic pre-pubertal predator-odor exposure and puberty evaluation**

134 Female pups were weaned on pnd 21 and separated into control and test groups. To investigate
135 the effects of chronic pre-pubertal psychosocial stress mice were removed from their home
136 cages, singly housed in new cages and left to habituate for 10 min. After the habituation period,
137 the mice were exposed to 12 µl of 2,4,5-Trimethylthiazole (TMT; synthetic extract of fox urine;
138 ≥98% purity; Sigma-Aldrich, UK) pipetted on a small circular piece of filter paper in a petri
139 dish placed in the centre of the cage for 20 min. The mice were exposed to TMT daily, at
140 random time points, for 14 days (from pnd 21 to 35). Control mice were exposed to filter paper
141 soaked with 12 µl of ddH_2O water. To rule out the possibility that physiological and
142 behavioural responses in TMT-exposed mice resulted from novelty of scent we repeated the
143 experiment with 85 mM of ethyl vanillin (≥98% purity; Sigma-Aldrich UK) as a control scent
144 in a separate cohort of mice. Mice were monitored from pnd 24 for vaginal opening (VO) and
145 first estrous (FE) indicated by epithelial cell cornification. Once the occurrence of VO was
146 detected, vaginal smears were taken to determine the exact day of FE.

147 **Pre-pubertal blood sampling**

148 The effect of TMT exposure on pre-pubertal LH pulses was measured, on pnd 26 and 29. Mice
149 were handled twice daily for 10 min to habituate to tail-tip blood collection for at least 7 days
150 prior to blood sampling, as described previously (5). For LH measurement, 3 µl of blood was
151 collected every 5 min for 80 min. Blood sampling was performed on pnd 26 and 29 during the
152 period of daily TMT exposure (pnd 21-35). Blood samples were collected at least 2 h before
153 TMT-exposure on these days. Blood collection was performed between 09:00-12:00 h.

154 For Ucn3 DREADDs experiments, blood sampling was performed on pnd 29 during the period
155 of daily CNO administration (pnd 21-35), as described above. Blood collection was performed
156 between 09:00-12:00 h.

157 **Behavioural tests**

158 ***Light Dark Box***

159 The same cohort of C57Bl6/J female mice were transported to a new room (lights off) and left
160 to habituate for 30 min. Mice were placed in the centre of the light compartment facing towards
161 the dark compartment. The time spent in each compartment (entry with all 4 limbs) was
162 recorded manually over a period of 5 min by two independent observers. The LDB test was
163 carried out on pnd 19, 27 and 40. Behaviour testing performed during the period of daily TMT
164 exposure (pnd 21-35) and was measured before the exposure to TMT on that day. This applies
165 to all behaviour tests performed during the TMT exposure period. All behaviour tests were
166 performed between 11:00-13:00 h.

167 ***Social interaction with familiar conspecific***

168 The same cohort of C57Bl6/J female mice were transported to a new dimly lit room and left to
169 habituate for 30 min. Experimental mice and a same sex familiar conspecific (similar age,
170 weight and strain) were placed simultaneously into the test arena (a new cage with clean wood-
171 chip bedding). The time spent following, sniffing, grooming and mounting the conspecific was
172 monitored and recorded manually over a period of 5 min by two independent observers. The
173 social interaction test was carried out on pnd 19, 27 and 40.

174 ***Elevated Plus maze***

175 The same cohort of C57Bl6/J female mice were transported to a new room (lights on) and left
176 to habituate for 30 min. Mice were placed in the centre of the maze facing towards the closed
177 arms. The time spent in each part of the maze (open, centre and closed; entry with all 4 limbs)
178 was recorded manually over a period of 5 min by two independent observers. The EPM test
179 was carried out on pnd 20, 28 and 41.

180 **Chronic DREADD activation of Ucn3 neurons in the MePD**

181 For DREADDs experiments, stock solution of Clozapine-N-oxide (CNO) (Tocris Bio-techne,
182 Abingdon, UK) was made by dissolving 5 mg of CNO in 1 ml of 0.9% sterile saline solution
183 and stored at 4 °C. CNO was made fresh daily and administered via drinking water at a final
184 concentration of 0.5 mg CNO/ kg, as described previously (32) for 14 days from pnd 21-35.
185 Mice were monitored from pnd 22 for vaginal opening (VO) and first estrous (FE), as described
186 above.

187 **Validation of AAV injection**

188 On pnd 50, Ucn3-cre-tdTomato mice were anaesthetised with a lethal dose of ketamine.
189 Transcardial perfusion was performed with heparinised saline for 5 min followed by ice-cold
190 4% paraformaldehyde (PFA) in phosphate buffer (pH 7.4) for 15 min with a pump (Minipuls,
191 Gilson, Villiers Le Bel, France). Brains were immediately collected and fixed in 15% sucrose
192 in 4% PFA at 4 °C and left to sink. Brains were then transferred to 30% sucrose in phosphate-
193 buffered saline (PBS) and left to sink. Brains were snap-frozen in isopropanol on dry ice and
194 stored in -80°C. Every third coronal brain section, 30-µm/section, was collected using a
195 cryostat (Bright Instrument Co., Luton, UK) through-out the MePD region corresponding to -
196 1.34 mm to -2.70 mm from bregma. Brain sections were mounted on microscope slides, air
197 dried and covered with ProLong Antifade mounting medium (Molecular Probes, Inc. OR,
198 USA). The number of tdTomato labelled and AAV-hM3D-mCitrine infected Ucn3 neurons
199 per side per slice in the MePD was quantified from 4 slices. For AAV-hM3D-mCitrine injected
200 Ucn3-cre-tdTomato mice we determined whether Ucn3 neurons were infected in the MePD
201 region by merging td-Tomato fluorescence of Ucn3 neurons with mCitrine fluorescence in the
202 MePD. Images were taken using Axioskop 2 Plus microscope (Carl Zeiss) equipped with

203 axiovision, version 4.7 (Carl Zeiss). Only data from animals with correct AAV injection were
204 analysed.

205 **LH pulse detection and analysis**

206 Blood samples were processed with a LH ELISA, as previously reported (33). Capture
207 antibody (monoclonal antibody, anti-bovine LHβ subunit, AB_2665514) was purchased from
208 Department of Animal Science at the University of California, Davis. Mouse LH standard
209 (AFP-5306A) and primary antibody (polyclonal antibody, rabbit LH antiserum, AB_2665533)
210 were obtained from Harbour-UCLA (California, USA). Secondary antibody (Horseradish-
211 Peroxidase (HRP)-linked donkey anti-rabbit IgG polyclonal antibody, AB_772206) was
212 purchased from VWR International (Leicestershire, UK). Inter-assay and intra-assay
213 variations were 4.6% and 10.2%, respectively and the assay sensitivity was 0.0015 ng/mL.
214 ODs of the standards were plotted against the log of the standard concentrations, non-linear
215 regression to fit the points and parameters were extracted to calculate the concentration of LH
216 (ng/ml) in blood samples, as previously described (33). The LH concentration at every time
217 point of blood collection was plotted as a line and scatter graph using Igor Pro 7, Wavemetrics,
218 Lake Oswego, OR, USA. DynPeak algorithm was used for the detection of LH pulses (34).

219 **Statistics**

220 For TMT-exposed and DREADD injected female pre-pubertal mice, data obtained for VO and
221 FE was analysed using RM one-way ANOVA. Data obtained for performance on LDB, SI and
222 EPM, LH pulse frequency and body weight measure were analysed using RM two-way
223 ANOVA. Statistics were performed using Igor Pro 7, Wavemetrics, Lake Oswego, OR, USA.
224 Data was represented as mean ± SEM and +$p<0.05$, ++$p<0.001$ and +++$p<0.0001$ were
225 considered to be significant.

226 **Results**

227 **Chronic TMT exposure delays puberty onset**

228 TMT exposure during the pubertal transition period, pnd 21 to 35, delayed FE without altering
229 VO compared water and ethyl vanillin controls in C57Bl6/J female mice (Fig. 1, A and B;
230 Control vs TMT, +++p<0.0001; TMT, n=14, water control, n=6, ethyl vanillin control, n=4).
231 Data for water and ethyl vanillin exposed control mice were combined as control since there
232 was no significant difference between the two control groups. Body weight was unaffected
233 between the experimental groups (Fig. 1, C; Control vs TMT). The data from this study shows
234 that predator-odor stress exposure during the pubertal transition delays pubertal onset.

235 **Chronic TMT exposure decreases pre-pubertal LH pulse frequency**

236 TMT exposure during the pubertal transition period, pnd 21 to 35, suppressed pre-pubertal LH
237 pulse frequency on pnd 26 and 29 compared to water and ethyl vanillin controls in C57Bl6/J
238 female mice (Fig. 2, A-E; Control vs TMT, ++p<0.001; TMT, n=8, water control, n=6, ethyl
239 vanillin control, n=3). On pnd 29, the average LH pulse frequency for the control group tended
240 to increase compared to the control group on pnd 26 potentially marking an acceleration of
241 GnRH pulse generator activity approaching the onset of puberty (Fig. 2, A, C and E). The
242 results of this experiment are summarised in the figure 2E. Data for water and ethyl vanillin
243 exposed control mice were combined as control since there was no significant difference
244 between the two control groups. The data from this study shows that predator-odor stress
245 exposure during the pubertal transition inhibits pre-pubertal LH pulsatility.

246 **Chronic TMT exposure induced long-lasting anxiety and fear-like behaviour**

247 We investigated anxiety and fear-like behaviour induced by TMT-exposure during the pubertal
248 transition period, pnd 21 to 35 in in C57Bl6/J female mice. Anxiety and fear-behaviour were

249 assessed using standard anxiety and fear tests, the LDB, SI and EPM, on pnd 19 or 20 (prior to
250 day of weaning and TMT-exposure), pnd 27 or 28 (during the TMT exposure period) and pnd
251 40 or 41 (a week after termination of TMT-exposure). The first LDB, SI and EPM trial on pnd
252 19 or 20, prior to weaning, confirms no group difference in anxiety before the beginning of
253 TMT-exposure (Fig. 3, A-C). TMT-exposed mice spent significantly less time in the light
254 compartment of the LDB as well as socialising with a familiar conspecific compared to the
255 control group on pnd 27, but not on pnd 40 (Fig. 3, A, B; Control vs TMT, +$p<0.05$; TMT,
256 n=14, water control, n=6, ethyl vanillin control, n=4). TMT-exposed mice spent less time in
257 the open arms of the EPM on pnd 28 and pnd 41 compared to controls (Fig. 3, C; Control vs
258 TMT, ++$p<0.001$; TMT, n=14, water control, n=6, ethyl vanillin control, n=4). It is
259 acknowledged that repeat testing on the EPM assesses phobia/fear (35). On pnd 20, pnd 28
260 and 41, within-group analysis showed no significant differences in the total time spent in the
261 open arms of the EPM across the different test days in the control group. However, within-
262 group analysis of the TMT-exposed group showed a significant difference in time-spent in the
263 open arm of the EPM on pnd 41 compared to pnd 28 (Fig. 3, C; TMT on pnd 28 vs TMT on
264 pnd 41, ###$p<0.0001$). TMT-exposure during pubertal transition had a long-lasting effect on
265 anxiety and fear/phobia.

266 **Selective expression of DREAD(Gq) in MePD Ucn3 neurons**

267 Evaluation of m-Citrine, hM3D, expression in tdTomato labelled neurons from AAV-injected
268 Ucn3-cre-tdTomato mice revealed that 86 ± 5% of MePD Ucn3 neurons expressed hM3D and
269 the number of tdTomato labelled Ucn3 neurons per side per slice in the MePD was counted at
270 72.90 ± 5.48 (mean ± SEM) with the number of AAV-hM3D-mCitrine infected neurons being
271 63.00 ± 6.83 (mean ± SEM) (n=8). A representative example is shown in Fig 4, A-F.

272 **Selective DREADD activation of Ucn3 neurons in the MePD delays puberty onset**

273 Bilateral DREADD activation of MePD Ucn3 neurons during the pubertal transition period,
274 pnd 21 to 35, of Ucn3-cre-tdTomato mice delayed FE without altering VO compared to non-
275 surgery and AAV-YFP controls (Fig. 5, A and B; Control vs DREADD, +$p<0.05$; DREADD,
276 n=8, control AAV, n=6, cre-negative control, n=4, no CNO, n=3). Data for cre-negative
277 control, no CNO and control AAV-YFP injected mice were combined as control since there
278 was no significant difference between the control groups. Body weight was unaffected
279 between the experimental groups (Fig. 5, C; Control vs DREADD). These data show that
280 activation of MePD Ucn3 during the pubertal transition delays pubertal timing. Mice with
281 misplaced injections (n=1) were excluded from the analysis.

282 **DREADD activation of Ucn3 neurons in the MePD suppresses pre-pubertal LH pulse**
283 **frequency**

284 Bilateral DREADD activation of MePD Ucn3 neurons during the pubertal transition period,
285 pnd 21 to 35, of Ucn3-cre-tdTomato mice suppressed pre-pubertal LH pulse frequency sampled
286 on pnd 29 compared to controls (Fig. 6, A, B and C; Control vs DREADD, +$p<0.05$; DREADD,
287 n=5, control AAV, n=3, cre-negative control, n=3). Data for cre-negative control and control
288 AAV-YFP injected mice were combined as control since there was no significant difference
289 between the control groups. These data show that activation of MePD Ucn3 during pubertal
290 transition suppresses pre-pubertal pulsatile LH secretion. Mice with misplaced injections
291 (n=1) were excluded from the analysis.

292 **Discussion**

293 The present study shows for the first time that chronic exposure to the psychogenic stressor,
294 predator odor, from pnd 21 for 14 days suppresses the pubertal acceleration of LH pulse

295 frequency, delaying puberty onset, while concurrently inducing long-lasting anxiety and fear-
296 like behaviour. Moreover, DREADD activation of MePD Ucn3 neurons during this same
297 developmental period delays puberty onset while suppressing pre-pubertal LH pulse frequency,
298 demonstrating that MePD Ucn3 signalling may play an important role in stress-related changes
299 in pubertal timing.

300 Hypothalamic kiss1 signalling is pivotal in regulating puberty onset in various species,
301 including rodents and humans (7,11). Pubertal onset is thought to be timed by an increase in
302 GnRH pulse generator frequency, however the mechanisms underlying the timing of ARC
303 kiss1 neuronal activation to trigger pubertal onset are not well established. Nevertheless,
304 puberty onset has been associated with increased ARC Tac2 (encoding NKB) and kiss1 mRNA
305 expression in mice (36,37), which are critical components of the GnRH pulse generator and
306 there is an increase in ARC kiss1 promoter activity during pubertal development (38). The
307 amygdala is known to influence pubertal timing in primates (17), and more specifically, the
308 MePD has been shown to regulate pubertal timing and reproductive function in rodents (4,19),
309 vis-à-vis MePD kiss1 receptor antagonism delays puberty, reduces the occurrence of
310 preovulatory LH surges in rats (25) and MePD kiss1 neuronal activation heightens sexual
311 partner preference in male mice (39). Recently, we have shown optogenetic stimulation of
312 MePD kiss1 neurons increases GnRH pulse generator frequency in adult female mice (26) and
313 preliminary data from our lab shows that activation of MePD kiss1 neurons during pubertal
314 transition advances the onset of first estrous, thus MePD kiss1 neurons may be an upstream
315 regulator of pubertal timing (40).

316 We explored the effect of chronic psychological stress exposure on pubertal timing, pre-
317 pubertal GnRH pulse generator activity and anxiety-like behaviour. Stress exposure during the
318 juvenile period is known to alter pubertal timing and induce anxiety behaviour in mammals,
319 including rodents, primates and humans (1,2,4,41). Predator odor exposure in rodents is a

320 model for PTSD; increasing fear and anxiety behaviour as well as reducing social interaction
321 (3). Previously, we have shown that acute TMT exposure suppresses LH pulsatility (5) and
322 restraint stress, another psychological stressor, inhibits LH pulse frequency while reducing
323 ARC kiss1 cfos expression in adult mice (42). Moreover, we have shown that cat odor delays
324 puberty and induces a fear response in rats (4). In the present study we show that the predator
325 odor, TMT, reduces LH pulsatility and delays the first estrous in female mice. In mice, VO
326 and FE do not coincide, wherein VO is not tightly coupled to the first ovulation, but rather a
327 variable time gap exists between VO and FE; the latter associated with first ovulation and
328 considered the unequivocal marker of puberty in this species (43). Additionally, pre-pubertal
329 LH pulse frequency in the control group tended to increase potentially marking the acceleration
330 of the GnRH pulse generator as the time of puberty onset approaches. Contrastingly, pre-
331 pubertal LH pulse frequency in the TMT-exposed group was significantly lower compared to
332 controls and we did not observe an increase in GnRH pulse generator activity between pnd 26
333 and 29.

334 Puberty is a sensitive period where enhanced neuroplasticity provides a context for the impact
335 of stress on the development of long-term anxiety disorders in humans (44). Early-life stress
336 increases anxiety-like behaviour in juvenile and adult mice linked to hyper-connectivity
337 between fronto-limbic circuits, involving the amygdala (45). The medial amygdala is activated
338 in response to external stressors and electrophysiological recordings reveal that predator urine
339 robustly activates the MePD, which is associated with delaying pubertal onset (4) and
340 supressing LH pulsatility in rodents (5,46). We found that predator odor-induced pubertal
341 delay was accompanied by increased anxiety-like behaviour, with mice spending significantly
342 less time in the light compartment of the LDB and in the open arms of the EPM during stress
343 exposure. Moreover, we observed that mice exposed to TMT exhibited long lasting fear-like
344 behaviour where they spent significantly less time in the open arm of the EPM compared to

345 controls on pnd 41; 6 days after termination of stress exposure. This is consistent with our
346 previous studies showing rats exposed to cat odor during pubertal development display
347 increased long-lasting fear-like behaviour on the EPM even after the termination of stress
348 exposure (4). Moreover, exposure to fox odor induces long-lasting anxiety on the EPM in rats
349 (47), while mice exposed to foot-shock stress during adolescence exhibit increased startle
350 reflexes into adulthood indicative of lasting anxiety-like behaviour (48). Additionally, TMT-
351 exposed mice showed significantly reduced social interaction with familiar con-specifics
352 during stress exposure whereas sociability tended to increase along with reproductive
353 maturation in the control group, which is consistent with our previous observations where
354 exposure to cat odor during puberty decreased sociability in rats (4).

355 Central administration of CRF inhibits kiss1 expression in the ARC and POA in rats (49). In
356 women with functional hypothalamic amenorrhea there is a correlation between decreased
357 serum kisspeptin and increased CRF concentrations (50). Moreover, an endogenous CRF tone
358 regulates pubertal timing where central administration of CRF in pnd 28 rats delays puberty
359 onset and administration of astressin-B, a CRFR1 antagonist, advances puberty (28). Central
360 antagonism of CRFR2 blocks the suppressive effect of stress on LH pulsatility in rodents (51).
361 These data indicate stress neuropeptides may provide an inhibitory tone on the timing of
362 puberty. Predator odor activates CRFR2 positive neurons in the medial amygdala of rats (52)
363 and we have recently shown that TMT-induced suppression of LH pulsatility is mediated by
364 MePD Ucn3 and CRFR2 signalling in mice (5). In the present study, selective activation of
365 MePD Ucn3 neurons during pubertal development delayed puberty and suppressed pre-
366 pubertal LH pulse frequency, demonstrating that MePD Ucn3 signalling plays a key role in
367 regulating pubertal timing.

368 The MePD has a major GABAergic output to key hypothalamic reproductive nuclei (21,53)
369 and we know the amygdala exerts an inhibitory brake on pubertal timing (17,19). Ucn3

370 neurons in the medial amygdala have an interneuron-like appearance (54) where Ucn3 fibres
371 overlap with CRFR2 expression (55,56) and we have shown that antagonism of MePD CRFR2
372 blocks the suppressive effect of TMT on LH pulse frequency in adult mice (5), thus Ucn3
373 neurons possibly connect to and signal via CRFR2 within the MePD. Moreover, the majority
374 of MePD CRFR2 neurons co-express GAD65 and 67 (29) indicating they are GABAergic and
375 may be involved in mediating stress-induced suppression of the GnRH pulse generator (22,53).
376 Therefore, MePD Ucn3 neurone activation may modulate pubertal timing possibly via
377 enhancing GABAergic output to inhibit GnRH pulse generator activity (5,21,23).

378 Our findings show for the first time that early life exposure to a psychosocial stressor disrupts
379 GnRH pulse generator frequency to delay puberty, and Ucn3 signalling in the MePD may be
380 involved in mediating this response. These findings provide novel insight into the key
381 interactions between the emotional stress centres and reproductive centres in the brain that
382 control pubertal onset in response to the external environment. Alterations in the timed onset
383 of puberty has major implications later in life with increased risk of diverse adverse outcomes,
384 including cancer, gynaecologic/obstetric, cardio-metabolic and neuro-cognitive categories in
385 humans (57). Understanding the mechanisms involved in controlling pubertal timing and the
386 impact of stress is crucial to ultimately aid future development of more effective treatments for
387 stress-related disorders of puberty.

388 **Acknowledgements**

389 The authors gratefully acknowledge the financial support from UKRI: BBSRC
390 (BB/S000550/1) and MRC (MR/N022637/1). DI is a PhD student funded by MRC-DTP
391 studentship at King's College London.

Funding

Grants supporting paper: Financial support from UKRI: BBSRC (BB/S000550/1) and MRC (MR/N022637/1). DI is a PhD student funded by MRC-DTP studentship at King's College London.

Conflict of Interest

The authors declare that the research was conducted in the absence of any commercial or financial relationships that could be construed as a potential conflict of interest.

Data Availability Statement

The original contributions presented in the study are included in the article/supplementary material. Further inquiries can be directed to the corresponding author.

Ethics Statement

The animal study was reviewed and approved by the Animal Welfare and Ethical Review Body Committee at King's College London.

Bibliography

1. Ponnapakkam A, Gensure R. Effects of stress after Hurricanes Katrina and Rita on pubertal disorders in children. Ochsner J. 2008;8(3):129–33.
2. Gur RE, Moore TM, Rosen AF, Barzilay R, Roalf DR, Calkins ME, Ruparel K, Scott JC, Almasy L, Satterthwaite TD, Shinohara RT . Burden of Environmental Adversity Associated with Psychopathology, Maturation, and Brain Behavior Parameters in Youths. JAMA Psychiatry. 2019;76(9):966–75.
3. Zoladz PR, Diamond DM . Predator-based psychosocial stress animal model of PTSD:

413 Preclinical assessment of traumatic stress at cognitive, hormonal, pharmacological,
414 cardiovascular and epigenetic levels of analysis. Exp Neurol. 2016;284(Pt B):211–9.
415 4. Li XF, Adekunbi DA, Alobaid HM, Li S, Pilot M, Lightman SL, O'Byrne KT . Role
416 of the posterodorsal medial amygdala in predator odour stress-induced puberty delay
417 in female rats. J Neuroendocrinol. 2019;31(6):e12719.
418 5. Ivanova D, Li XF, McIntyre C, Liu Y, Kong L, O'Byrne KT . Urocortin3 in the
419 Posterodorsal Medial Amygdala Mediates Stress-induced Suppression of LH
420 Pulsatility in Female Mice. Endocrinology. 2021;162(12):bqab206.
421 6. Wagenmaker ER, Moenter SM. Exposure to acute psychosocial stress disrupts the
422 luteinizing hormone surge independent of estrous cycle alterations in female mice.
423 Endocrinology. 2017;158(8):2593–602.
424 7. Terasawa E, Guerriero KA, Plant TM. Kisspeptin and Puberty in Mammals. Adv Exp
425 Med Biol. 2013;784:253–73.
426 8. De Roux N, Genin E, Carel JC, Matsuda F, Chaussain JL, Milgrom E.
427 Hypogonadotropic hypogonadism due to loss of function of the KiSS1-derived peptide
428 receptor GPR54. Proc Natl Acad Sci U S A. 2003;100(19):10972–6.
429 9. Seminara SB, Messager S, Chatzidaki EE, Thresher RR, Acierno Jr JS, Shagoury JK,
430 Bo-Abbas Y, Kuohung W, Schwinof KM, Hendrick AG, Zahn D . The GPR54 gene as
431 a regulator of puberty. N Engl J Med. 2003;349(17):1614–27.
432 10. Plant TM, Ramaswamy S, DiPietro MJ. Repetitive activation of hypothalamic G
433 protein-coupled receptor 54 with intravenous pulses of kisspeptin in the juvenile
434 monkey (Macaca mulatta) elicits a sustained train of gonadotropin-releasing hormone
435 discharges. Endocrinology. 2006;147(2):1007–13.
436 11. Navarro VM, Fernandez-Fernandez R, Castellano JM, Roa J, Mayen A, Barreiro ML,
437 Gaytan F, Aguilar E, Pinilla L, Dieguez C, Tena-Sempere M . Advanced vaginal

438 opening and precocious activation of the reproductive axis by KiSS-1 peptide, the
439 endogenous ligand of GPR54. J Physiol. 2004;561(2):379–86.
440 12. Clarkson J, Han SY, Piet R, McLennan T, Kane GM, Ng J, Porteous RW, Kim JS,
441 Colledge WH, Iremonger KJ, Herbison AE. Definition of the hypothalamic GnRH
442 pulse generator in mice. Proc Natl Acad Sci U S A. 2017;114(47):e10216–23.
443 13. Qiu J, Nestor CC, Zhang C, Padilla SL, Palmiter RD, Kelly MJ, Rønnekleiv OK .
444 High-frequency stimulation-induced peptide release synchronizes arcuate kisspeptin
445 neurons and excites GnRH neurons. Elife. 2016;5:e16246.
446 14. Voliotis M, Li XF, De Burgh R, Lass G, Lightman SL, O'Byrne KT, Tsaneva-
447 Atanasova K . The Origin of GnRH pulse generation: An integrative mathematical-
448 experimental approach. J Neurosci. 2019;39(49):9738–47.
449 15. Liu X, Yeo SH, McQuillan HJ, Herde MK, Hessler S, Cheong I, Porteous R, Herbison
450 AE . Highly redundant neuropeptide volume co-transmission underlying episodic
451 activation of the gnrh neuron dendron. Elife. 2021;10:e62455.
452 16. Wang L, Moenter SM. Differential Roles of Hypothalamic AVPV and Arcuate
453 Kisspeptin Neurons in Estradiol Feedback Regulation of Female Reproduction.
454 Neuroendocrinology. 2020;110(3–4):172–84.
455 17. Stephens SBZ, Raper J, Bachevalier J, Wallen K. Neonatal amygdala lesions advance
456 pubertal timing in female rhesus macaques. Psychoneuroendocrinology. 2015;51:307–
457 17.
458 18. Bar-Sela M, Critchlow V. Delayed puberty following electrical stimulation of
459 amygdala in female rats. Am J Physiol. 1966;211(5):1103–7.
460 19. Li XF, Hu MH, Hanley BP, Lin YS, Poston L, Lightman SL, O'Byrne KT . The
461 posterodorsal medial amygdala regulates the timing of puberty onset in female rats.
462 Endocrinology. 2015;156(10):3725–36.

463 20. Choi GB, Dong HW, Murphy AJ, Valenzuela DM, Yancopoulos GD, Swanson LW,
464 Anderson DJ . Lhx6 delineates a pathway mediating innate reproductive behaviors
465 from the amygdala to the hypothalamus. Neuron. 2005;46(4):647–60.
466 21. Keshavarzi S, Sullivan RKP, Ianno DJ, Sah P. Functional properties and projections of
467 neurons in the medial amygdala. J Neurosci. 2014;34(26):8699–715.
468 22. Moore AM, Coolen LM, Lehman MN. Kisspeptin/Neurokinin B/Dynorphin (KNDy)
469 cells as integrators of diverse internal and external cues: evidence from viral-based
470 monosynaptic tract-tracing in mice. Sci Rep. 2019;9(1):1–5.
471 23. Yeo SH, Kyle V, Blouet C, Jones S, Colledge WH. Mapping neuronal inputs to Kiss1
472 neurons in the arcuate nucleus of the mouse. PLoS One. 2019;14(3):e0213927.
473 24. Kim J, Semaan SJ, Clifton DK, Steiner RA, Dhamija S, Kauffman AS. Regulation of
474 Kiss1 expression by sex steroids in the amygdala of the rat and mouse. Endocrinology.
475 2011;152(5):2020–30.
476 25. Adekunbi DA, Li XF, Li S, Adegoke OA, Iranloye BO, Morakinyo AO, Lightman SL,
477 Taylor PD, Poston L, O'Byrne KT . Role of amygdala kisspeptin in pubertal timing in
478 female rats. PLoS One. 2017;12(8):e0183596.
479 26. Lass G, Li XF, de Burgh RA, He W, Kang Y, Hwa-Yeo S, Sinnett-Smith LC,
480 Manchishi SM, Colledge WH, Lightman SL, O'Byrne KT . Optogenetic stimulation of
481 kisspeptin neurones within the posterodorsal medial amygdala increases luteinising
482 hormone pulse frequency in female mice. J Neuroendocrinol. 2020;32(2):e12823.
483 27. Govic A, Paolini AG. In vivo electrophysiological recordings in amygdala subnuclei
484 reveal selective and distinct responses to a behaviorally identified predator odor. J
485 Neurophysiol. 2015;113(5):1423–36.
486 28. Kinsey-Jones JS, Li XF, Knox AM, Lin YS, Milligan SR, Lightman SL, O'Byrne KT .
487 Corticotrophin-releasing factor alters the timing of puberty in the female rat. J

488 Neuroendocrinol. 2010;22(2):102–9.
489 29. Shemesh Y, Forkosh O, Mahn M, Anpilov S, Sztainberg Y, Manashirov S,
490 Shlapobersky T, Elliott E, Tabouy L, Ezra G, Adler ES . Ucn3 and CRF-R2 in the
491 medial amygdala regulate complex social dynamics. Nat Neurosci. 2016;19(11):1489–
492 96.
493 30. Jamieson PM, Li C, Kukura C, Vaughan J, Vale W. Urocortin 3 modulates the
494 neuroendocrine stress response and is regulated in rat amygdala and hypothalamus by
495 stress and glucocorticoids. Endocrinology. 2006;147(10):4578–88.
496 31. Paxinos G, Franklin KB . Mouse Brain in Stereotaxic Coordinates. Acad Press.
497 2019;5:246.
498 32. Zhan J, Komal R, Keenan WT, Hattar S, Fernandez DC . Non-invasive strategies for
499 chronic manipulation of dreadd-controlled neuronal activity. J Vis Exp.
500 2019;2019(150):e59439.
501 33. Steyn FJ, Wan Y, Clarkson J, Veldhuis JD, Herbison AE, Chen C. Development of a
502 methodology for and assessment of pulsatile luteinizing hormone secretion in juvenile
503 and adult male mice. Endocrinology. 2013;154(12):4939–45.
504 34. Vidal A, Zhang Q, Médigue C, Fabre S, Clément F. Dynpeak: An algorithm for pulse
505 detection and frequency analysis in hormonal time series. PLoS One.
506 2012;7(7):e39001.
507 35. Fernandes C, File SE. The influence of open arm ledges and maze experience in the
508 elevated plus-maze. Pharmacol Biochem Behav. 1996;54(1):31–40.
509 36. Gill JC, Navarro VM, Kwong C, Noel SD, Martin C, Xu S, Clifton DK, Carroll RS,
510 Steiner RA, Kaiser UB . Increased Neurokinin B (Tac2) Expression in the Mouse
511 Arcuate Nucleus Is an Early Marker of Pubertal Onset with Differential Sensitivity to
512 Sex Steroid-Negative Feedback than Kiss1. Endocrinology. 2012;153(10):4883.

513 37. Simavli S, Thompson IR, Maguire CA, Gill JC, Carroll RS, Wolfe A, Kaiser UB,
514 Navarro VM . Substance P Regulates Puberty Onset and Fertility in the Female
515 Mouse. Endocrinology. 2015;156(6):2313–22.
516 38. Wright H, Aylwin CF, Toro CA, Ojeda SR, Lomniczi A . Polycomb represses a gene
517 network controlling puberty via modulation of histone demethylase Kdm6b
518 expression. Sci Rep. 2021;11(1):1–7.
519 39. Adekunbi DA, Li XF, Lass G, Shetty K, Adegoke OA, Yeo SH, Colledge WH,
520 Lightman SL, O'Byrne KT. Kisspeptin neurones in the posterodorsal medial amygdala
521 modulate sexual partner preference and anxiety in male mice. J Neuroendocrinol.
522 2018;30(3):e12572.
523 40. Ivanova D, Li XF, McIntyre C, O'Byrne KT . Chronic Exposure to Predator Odour
524 Stress Disrupts LH Pulsatility and Delays Puberty While Activation of Amygdala
525 Kisspeptin Advances Puberty. Endocr Soc. 2020;Supplement:SUN-LB49.
526 41. Pincus M, Godfrey JR, Feczko E, Earl E, Miranda-Dominguez O, Fair D, Wilson ME,
527 Sanchez MM, Kelly C . Chronic psychosocial stress and experimental pubertal delay
528 affect socioemotional behavior and amygdala functional connectivity in adolescent
529 female rhesus macaques. Psychoneuroendocrinology. 2021;127:105154.
530 42. Yang JA, Song CI, Hughes JK, Kreisman MJ, Parra RA, Haisenleder DJ, Kauffman
531 AS, Breen KM . Acute psychosocial stress inhibits LH pulsatility and kiss1 neuronal
532 activation in female mice. Endocrinology. 2017;158(11):3716–23.
533 43. Gaytan F, Morales C, Leon S, Heras V, Barroso A, Avendaño MS, Vazquez MJ,
534 Castellano JM, Roa J, Tena-Sempere M . Development and validation of a method for
535 precise dating of female puberty in laboratory rodents: The puberty ovarian maturation
536 score (Pub-Score). Sci Rep. 2017;7(1):1–11.
537 44. Marshall AD . Developmental timing of trauma exposure relative to puberty and the

538 nature of psychopathology among adolescent girls. J Am Acad Child Adolesc
539 Psychiatry. 2016;55(1):25–32.
540 45. Johnson FK, Delpech JC, Thompson GJ, Wei L, Hao J, Herman P, Hyder F, Kaffman
541 A . Amygdala hyper-connectivity in a mouse model of unpredictable early life stress.
542 Transl Psychiatry. 2018;8(1):1–14.
543 46. Lin Y, Li XF, Lupi M, Kinsey-Jones JS, Shao B, Lightman SL, O'Byrne KT . The role
544 of the medial and central amygdala in stress-induced suppression of pulsatile LH
545 secretion in female rats. Endocrinology. 2011;152(2):545–55.
546 47. Dopfel D, Perez PD, Verbitsky A, Bravo-Rivera H, Ma Y, Quirk GJ, Zhang N .
547 Individual variability in behavior and functional networks predicts vulnerability using
548 an animal model of PTSD. Nat Commun. 2019;10(1):1–2.
549 48. Chester JA, Barrenha GD, Hughes ML, Keuneke KJ . Age- and sex-dependent effects
550 of footshock stress on subsequent alcohol drinking and acoustic startle behavior in
551 mice selectively bred for high-alcohol preference. Alcohol Clin Exp Res.
552 2008;32(10):1782–94.
553 49. Kinsey-Jones JS, Li XF, Knox AM, Wilkinson ES, Zhu XL, Chaudhary AA, Milligan
554 SR, Lightman SL, O'byrne KT . Down-regulation of hypothalamic kisspeptin and its
555 receptor, Kiss1r, mRNA expression is associated with stress-induced suppression of
556 luteinising hormone secretion in the female rat. J Neuroendocrinol. 2009;21(1):20–9.
557 50. Agnieszka Podfigurna, Anna Szeliga BM. Serum kisspeptin and corticotropin-
558 releasing hormone levels in patients with functional hypothalamic amenorrhea.
559 Gynecol Reprod Endocrinol Metab. 2020;1(1):37–42.
560 51. Li XF, Bowe JE, Lightman SL, O'Byrne KT . Role of corticotropin-releasing factor
561 receptor-2 in stress-induced suppression of pulsatile luteinizing hormone secretion in
562 the rat. Endocrinology. 2005;146(1):318–22.

563 52. Fekete ÉM, Zhao Y, Li C, Sabino V, Vale WW, Zorrilla EP. Social defeat stress
564 activates medial amygdala cells that express type 2 corticotropin-releasing factor
565 receptor mRNA. Neuroscience. 2009;162(1):5–13.
566 53. Pardo-Bellver C, Cádiz-Moretti B, Novejarque A, Martínez-García F, Lanuza E.
567 Differential efferent projections of the anterior, posteroventral, and posterodorsal
568 subdivisions of the medial amygdala in mice. Front Neuroanat. 2012;6(33):1–26.
569 54. Deussing JM, Breu J, Kühne C, Kallnik M, Bunck M, Glasl L, Yen YC, Schmidt MV,
570 Zurmühlen R, Vogl AM, Gailus-Durner V . Urocortin 3 modulates social
571 discrimination abilities via corticotropin-releasing hormone receptor type 2. J
572 Neurosci. 2010;30(27):9103–16.
573 55. Cavalcante JC, Sita LV, Mascaro MB, Bittencourt JC, Elias CF. Distribution of
574 urocortin 3 neurons innervating the ventral premammillary nucleus in the rat brain.
575 Brain Res. 2006;1089(1):116–25.
576 56. Li C, Vaughan J, Sawchenko PE, Vale WW. Urocortin III-immunoreactive projections
577 in rat brain: Partial overlap with sites of type 2 corticotrophin-releasing factor receptor
578 expression. J Neurosci. 2002;22(3):991–1001.
579 57. Day FR, Elks CE, Murray A, Ong KK, Perry JRB. Puberty timing associated with
580 diabetes, cardiovascular disease and also diverse health outcomes in men and women:
581 the UK Biobank study. Sci Rep. 2015;5(1):1–12.
582

583 **Figure 1.** Female C57Bl6/J mice chronically exposed to 2,4,5-Trimethylthiazole (TMT) from
584 post-natal day (pnd) 21 for 14 days showed delayed first estrous (FE) without affecting vaginal
585 opening (VO) and body weight (BW). Effect of chronic TMT exposure on day of VO (A), FE
586 (B) and (C) BW weight gain between pnd 21 and 45. +++$p<0.0001$ Control group (combined
587 water control: n=6; ethyl vanillin control: n=4) vs TMT group (n=14).

588 **Figure 2.** Female C57Bl6/J mice chronically exposed to 2,4,5-Trimethylthiazole (TMT) from
589 post-natal day (pnd) 21 for 14 days showed suppressed pre-pubertal pulsatile luteinising
590 hormone (LH) secretion on pnd 26 and 29. Representative LH pulse profile with (A) control
591 mouse on pnd 26, (B) TMT-exposed mouse on pnd 26, (C) control mouse on pnd 29 and (D)
592 TMT-exposed mouse on pnd 29. (E), Summary of LH pulse frequency on pnd 26 and 29 of
593 control and TMT-exposed group during the 80 min blood sampling period. LH pulses detected
594 by the DynePeak algorithm are indicated with an asterisk located above each pulse on the
595 representative LH pulse profiles. ++$p<0.001$ control group (combined water control: n=6;
596 ethyl vanillin control: n=3) vs. TMT-exposed group (n=8) on pnd 26 and 29.

597 **Figure 3.** Female C57Bl6/J mice chronically exposed to 2,4,5-Trimethylthiazole (TMT)
598 showed increased anxiety-like behavior on the light-dark box (LDB) and elevated plus maze
599 (EPM) and decreased social interaction with familiar conspecifics on the social interaction (SI)
600 test. (A) Summary of time spent in the light compartment of the LDB on post-natal day (pnd)
601 19 (before beginning of TMT-exposure), 27 (during TMT exposure) and 40 (after termination
602 of TMT-exposure), (B) time spent socially interacting with familiar conspecifics on pnd 19, 27
603 and 40, and (C) time spent in the open arm of the EPM on pnd 20, 28 and 41. +$p<0.05$ time
604 spent on LDB, SI and EPM of control group (combined water control: n=6; ethyl vanillin
605 control: n=4) vs TMT-exposed group (n=14) on pnd 27 or 28 (during TMT-exposure);
606 ###$p<0.0001$ time spent in the open arm of the EPM in the TMT-exposed group on pnd 28 vs
607 pnd 41.

608 **Figure 4.** Expression of AAV5-hSyn-DIO-HA-hM3D(Gq)-IRES-mCitrine in posterodorsal
609 medial amygdala (MePD) Urocortin 3 (Ucn3) neurons. (A-F) Representative dual fluorescence
610 photomicrographs of the MePD from a Ucn3-cre-tdTomato female mouse injected with
611 AAV5-hSyn-DIO-HA-hM3D(Gq)-IRES-mCitrine. Ucn3 neurons labelled with m-Citrine (A)

612 and tdTomato (C) appear yellow/orange (E). (B), (D) and (F) are a higher power view of (A),
613 (C) and (E) respectively. Scale bars represent A, C, E 100 μm and B, D, F 25 μm; OT, Optic
614 tract (blue line).

615 **Figure 5.** DREADD (hM3D) activation of urocortin 3 (Ucn3) neurons in the posterodorsal
616 sub-nucleus of the medial amygdala (MePD) of Ucn3-cre-tdTomato female mice from post-
617 natal day (pnd) 21 for 14 days delays first estrous (FE) without affecting vaginal opening (VO)
618 and body weight (BW) in urocortin3-cre-tdTomato female mice. Effect of MePD Ucn3
619 activation on day of VO (A), FE (B) and (C) BW weight gain between pnd 21 and 45. +$p<0.05$
620 Control group (combined control AAV: n=6; cre-negative control: n=4; no CNO n=3) vs
621 DREADD group (n=8).

622 **Figure 6.** DREADD (hM3D) activation of urocortin 3 (Ucn3) neurons in the posterodorsal
623 sub-nucleus of the medial amygdala (MePD) in Ucn3-cre-tdTomato female mice from post-
624 natal day (pnd) 21 for 14 days suppresses pre-pubertal LH pulse frequency sampled on pnd 29.
625 Representative LH pulse profile from Ucn3-cre-tdTomato female mice on pnd 29 with (A)
626 control mouse, (B) DREADD (hM3D) activated mouse, (C) Summary of LH pulse frequency
627 on pnd 29 of control and DREADD group during the 80 min blood sampling period. LH pulses
628 detected by the DynePeak algorithm are indicated with an asterisk located above each pulse on
629 the representative LH pulse profiles. +$p<0.05$ Control group (combined control AAV: n=3;
630 cre-negative control: n=3) vs DREADD group (n=5).

Figure 1

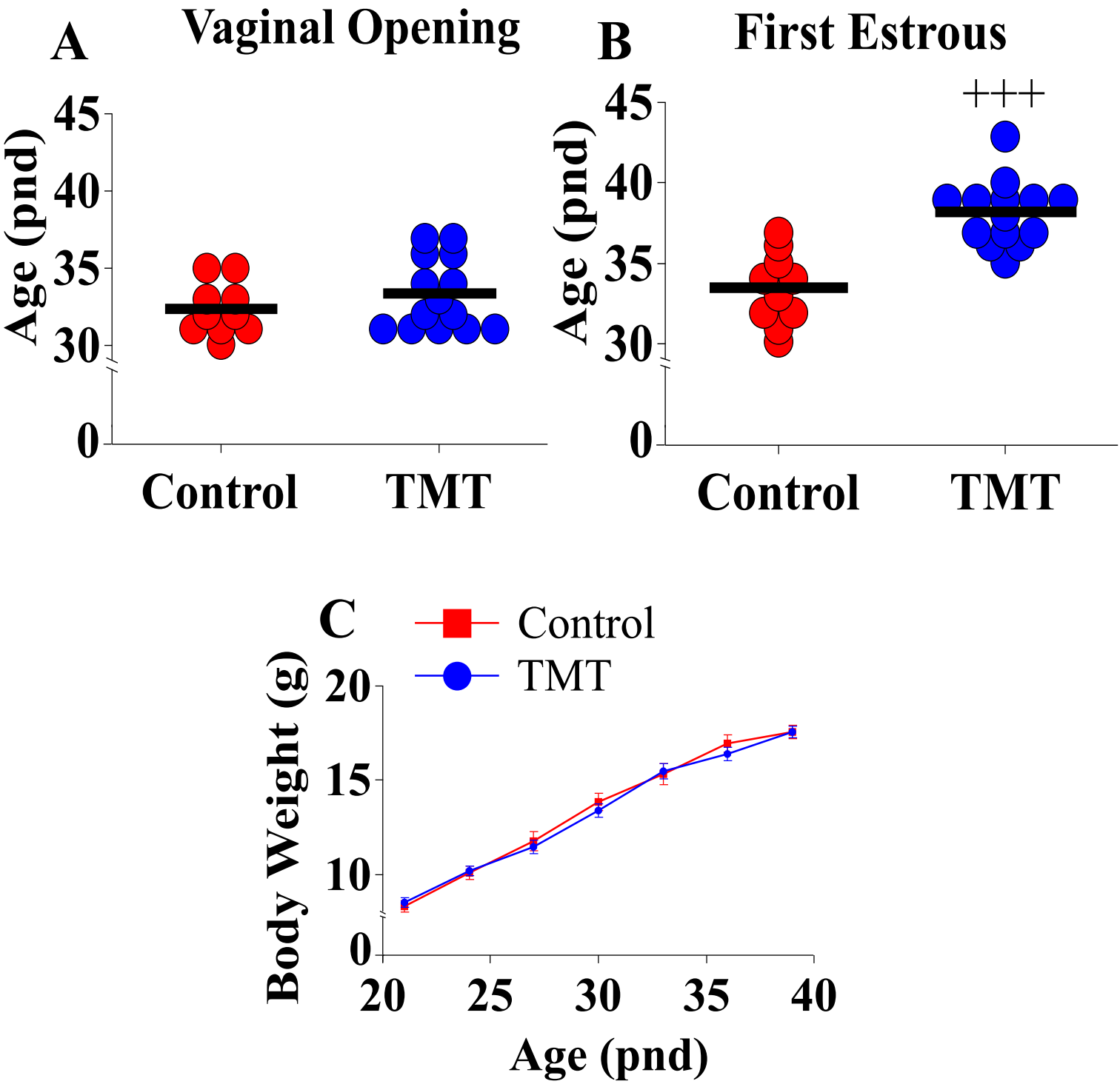
A
Vaginal Opening
Age (pnd)
45
40
35
30
0
Control
TMT
B
First Estrous
+++
Age (pnd)
45
40
35
30
0
Control
TMT
C
Control
TMT
Body Weight (g)
20
15
10
0
20
25
30
35
40
Age (pnd)

Figure 2

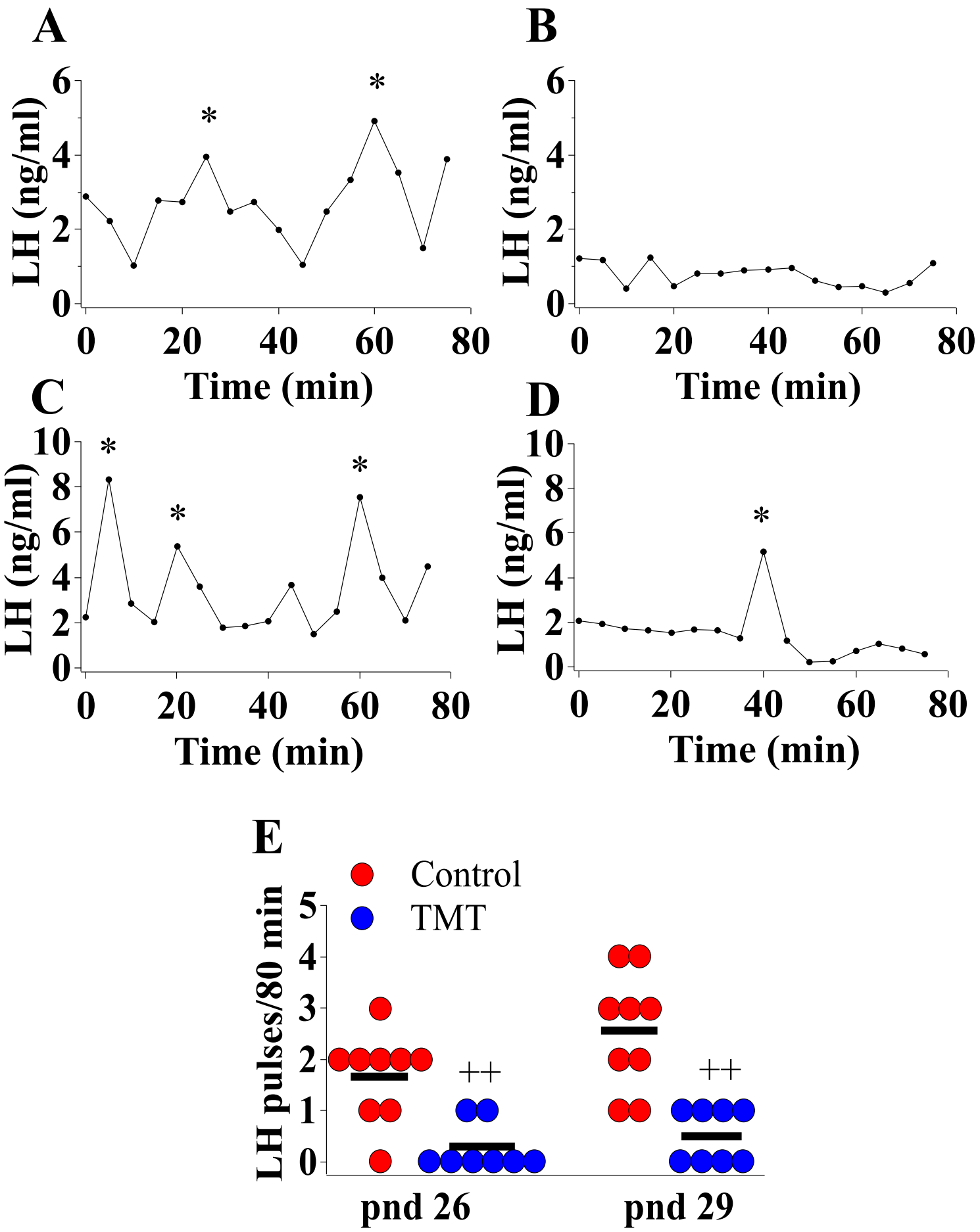
A
B
C
D
E
LH (ng/ml)
Time (min)
LH pulses/80 min
Control
TMT
++
pnd 26
pnd 29

Figure 3

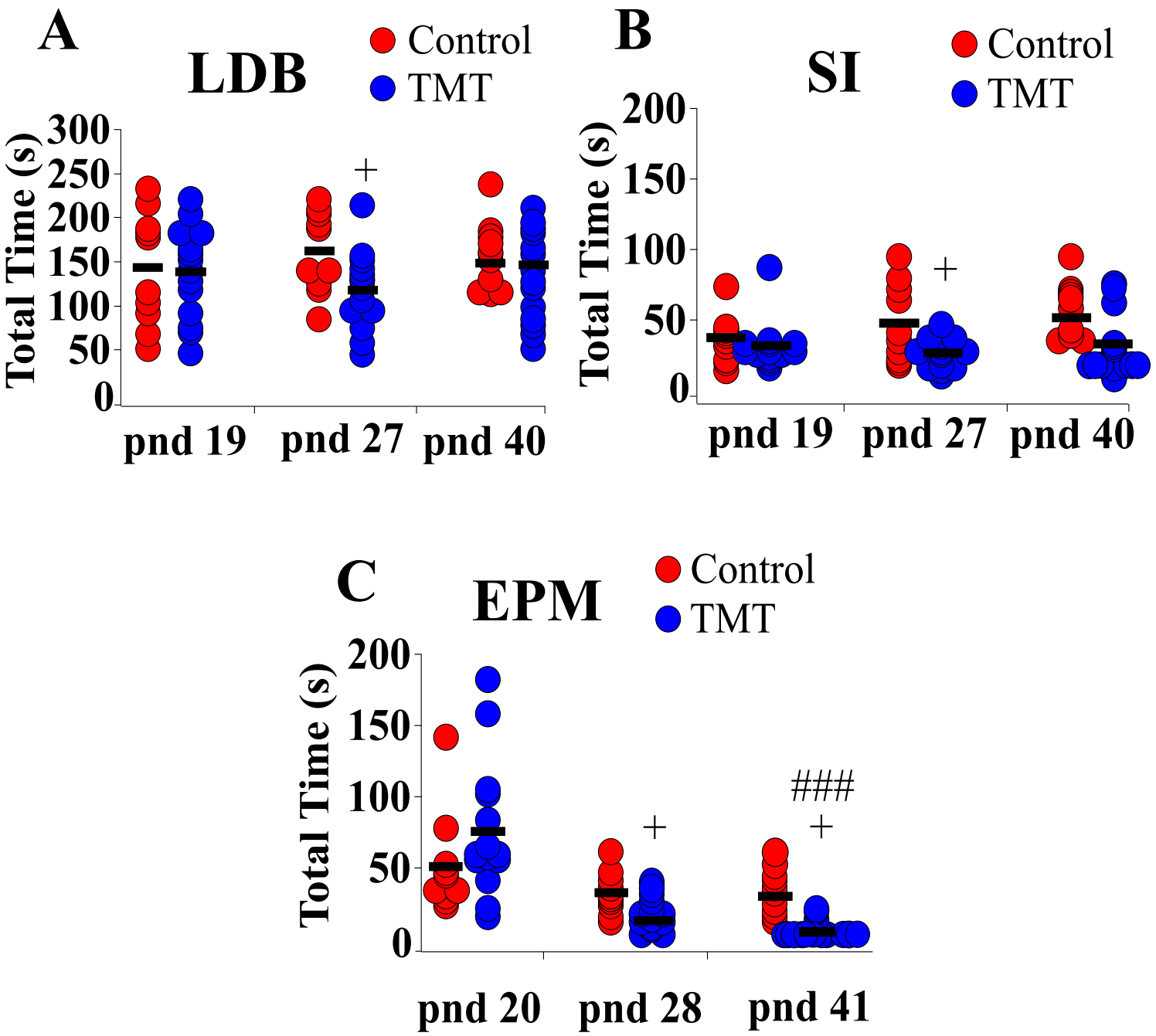
A
LDB
Control
TMT
Total Time (s)
300
250
200
150
100
50
0
+
pnd 19
pnd 27
pnd 40
B
SI
Control
TMT
Total Time (s)
200
150
100
50
0
+
pnd 19
pnd 27
pnd 40
C
EPM
Control
TMT
Total Time (s)
200
150
100
50
0
+
###
+
pnd 20
pnd 28
pnd 41

Figure 4

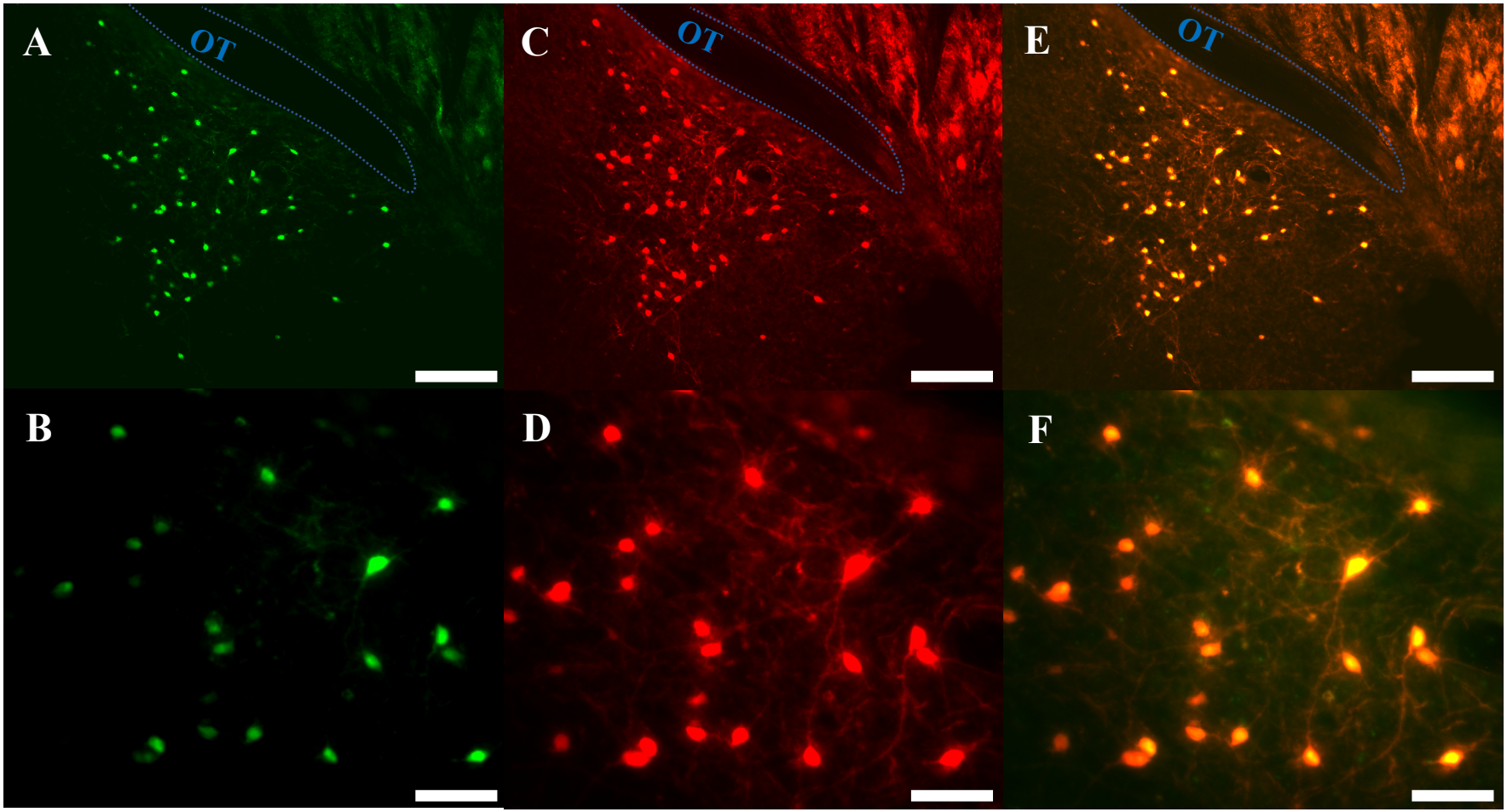

Figure 5

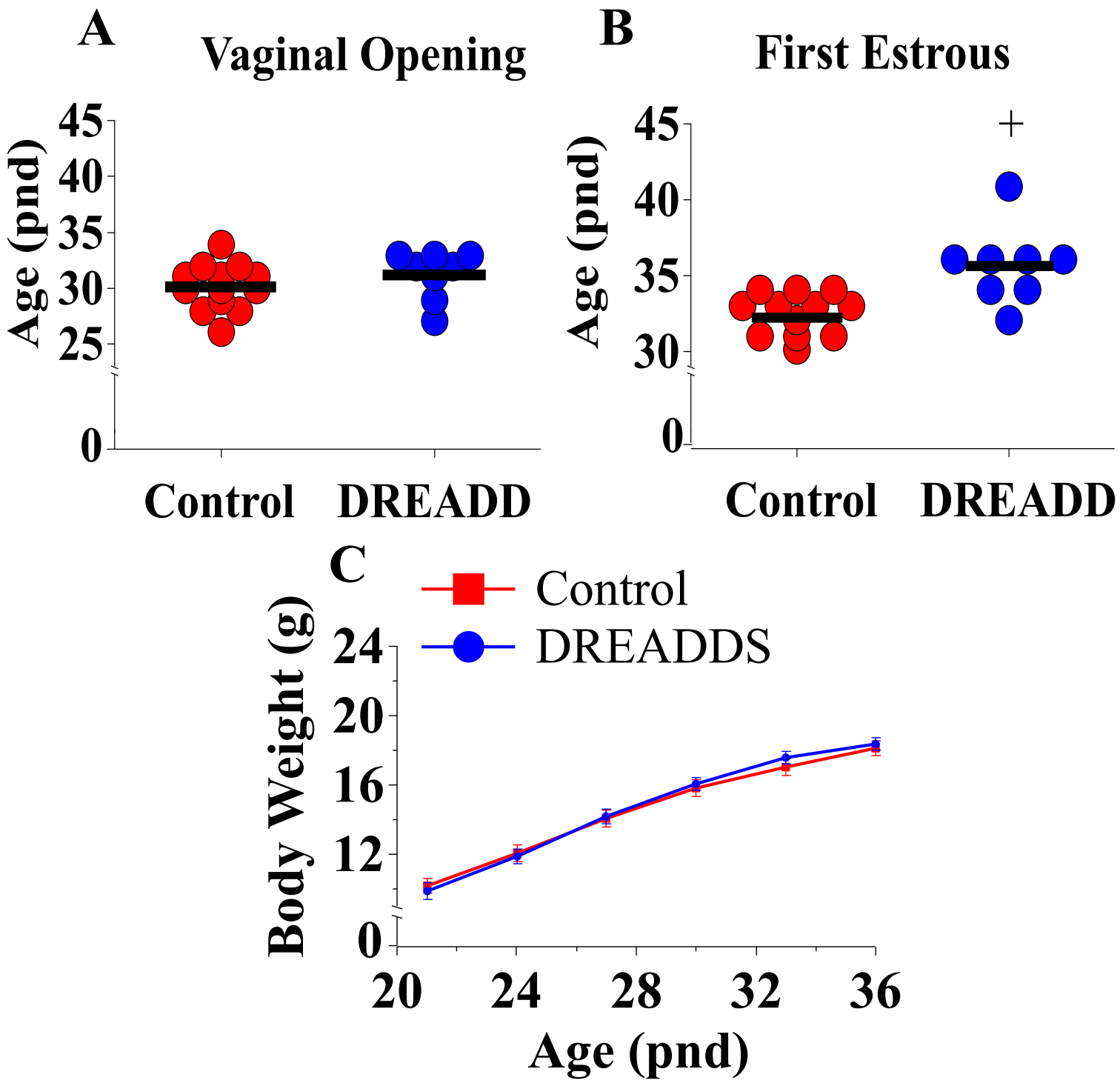
A
Vaginal Opening
Age (pnd)
45
40
35
30
25
0
Control
DREADD
B
First Estrous
Age (pnd)
45
40
35
30
0
+
Control
DREADD
C
Control
DREADDS
Body Weight (g)
24
20
16
12
0
20
24
28
32
36
Age (pnd)
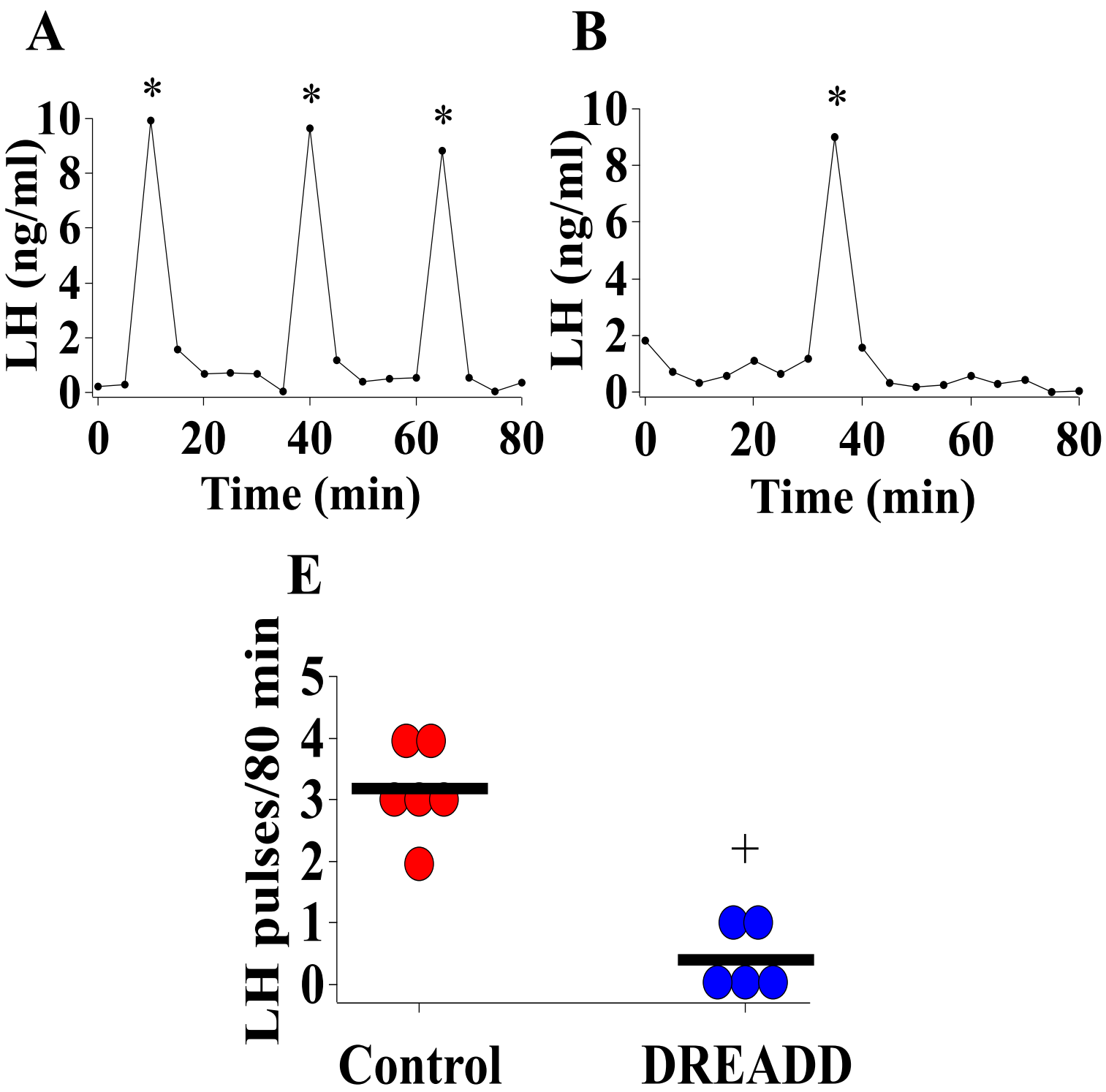
Figure 6